doi:10.1016/j.jmb.2005.05.001 J. Mol. Biol. (2005) 350, 611–616

JMB

Available online at www.sciencedirect.com

SCIENCE DIRECT®

ELSEVIER

COMMUNICATION

The 5 Å Structure of Heterologously Expressed Plant Aquaporin SoPIP2;1

W. Kukulski[1], A. D. Schenk[1], U. Johanson[2], T. Braun[1], B. L. de Groot[3] D. Fotiadis[1], P. Kjellbom[2] and A. Engel[1]*

[1]*Maurice E. Müller Institute for Microscopy, Biozentrum University of Basel, CH-4056 Basel, Switzerland*

[2]*Department of Plant Biochemistry, Lund University S-221 00 Lund, Sweden*

[3]*Computational Biomolecular Dynamics Group Max-Planck-Institute for Biophysical Chemistry, Am Fassberg 11, D-37077 Göttingen Germany*

**Corresponding author*

SoPIP2;1 is one of the major integral proteins in spinach leaf plasma membranes. In the *Xenopus* oocyte expression system its water channel activity is regulated by phosphorylation at the C terminus and in the first cytosolic loop. To assess its structure, SoPIP2;1 was heterologously expressed in *Pichia pastoris* as a His-tagged protein and in the non-tagged form. Both forms were reconstituted into 2D crystals in the presence of lipids. Tubular crystals and double-layered crystalline sheets of non-tagged SoPIP2;1 were observed and analyzed by cryo-electron microscopy. Crystalline sheets were highly ordered and diffracted electrons to a resolution of 2.96 Å. High-resolution projection maps of tilted specimens provided a 3D structure at 5 Å resolution. Superposition of the SoPIP2;1 potential map with the atomic model of AQP1 demonstrates the generally well conserved overall structure of water channels. Differences concerning the extracellular loop A explain the particular crystal contacts between oppositely oriented membrane sheets of SoPIP2;1 2D crystals, and may have a function in rapid volume changes observed in stomatal guard cells or mesophyll protoplasts. This crystal packing arrangement provides access to the phosphorylated C terminus as well as the loop B phosphorylation site for studies of channel gating.

Keywords: aquaporin; electron diffraction; electron microscopy; three-dimensional structure; two-dimensional crystals

Cytosolic osmoregulation is maintained at the single-cell level and whole-plant water homeostasis is an essential function for every plant. It is accomplished by a complex and only rudimentarily understood system. While long-distance water transport is fulfilled by the vascular tissue, the cells themselves provide a rapid short-distance water flow through membranes. Proteins of the aquaporin family are key components in cellular water homeostasis, and they account for a significant fraction of the total amount of integral membrane proteins of plant plasma membranes.[1] Their importance is demonstrated also by the fact that in *Arabidopsis* 35 genes encode expressed aquaporin-like proteins and around one-third of these are located at the plasma membrane.[2]

At the cellular level, the maintenance of the water balance is an interplay between plasma membrane and tonoplast aquaporins (plasma membrane intrinsic proteins (PIPs) and tonoplast intrinsic proteins (TIPs), respectively). The PIPs are subdivided into two groups, the PIP1 and PIP2 isoforms. The latter have a longer C-terminal region and, when expressed in *Xenopus* oocytes, show a higher water transport activity than the PIP1 isoforms.[3]

SoPIP2;1, in previous nomenclature called PM28A, is a PIP2 isoform in *Spinacia oleracea* (spinach) leaf plasma membranes, where aquaporins constitute ~20% of all integral membrane proteins.[4] In its C-terminal region, a serine residue was found to be phosphorylated *in vivo*, in response to increasing apoplastic water potential.[4] Results generated by using the *Xenopus* oocyte expression system in combination with site-directed

Abbreviations used: AQP, aquaporin; PIP, plasma membrane intrinsic protein; TIP, tonoplast intrinsic protein.

E-mail address of the corresponding author: andreas.engel@unibas.ch

mutagenesis suggested that phosphorylation at Ser274 in the C-terminal region regulates the water channel activity of SoPIP2;1.[5] Furthermore, another serine residue, Ser115, in a consensus phosphorylation site in the first cytosolic loop, i.e. loop B, was identified as an additional putative regulatory phosphorylation site.[5] A hypothetical model has been presented in which an osmosensor senses the difference and triggers the increase of the intracellular concentration of Ca^{2+} when the apoplastic water potential is higher than the water potential in the cell.[5,6] This leads to the activation of a plasma membrane-associated Ca^{2+}-dependent protein kinase, which phosphorylates SoPIP2;1 at the Ser274 residue and thus facilitates water influx. At low apoplastic water potential, the channel is dephosphorylated and water flow through the pore is restricted. The consensus phosphorylation site at Ser274 in the C-terminal region is conserved in all PIP2 isoforms, independent of species, but not in the PIP1 isoforms, which have a shorter C-terminal region. The consensus phosphorylation site in the loop B at Ser115 is conserved in all PIPs, i.e. in all PIP1 as well as PIP2 isoforms.[2]

Several aquaporin structures have been solved in the past few years; human AQP1,[7,8] AQP0 from sheep[9] and bovine[10] eye lens, as well as two bacterial members, GlpF[11] and AqpZ.[12] Together with molecular dynamics simulations,[13–17] these structures gave insight into function and selectivity of water channels. In the case of AQP0, clues about its specific pH-dependent regulation could be derived,[9] and the structures of the open[10] and closed[9] AQP0 water channel are now available. The only plant aquaporin for which structural data are available is a projection map of the vacuolar membrane aquaporin α-TIP determined by electron crystallography.[18] Thus, the density map presented here is the first 3D plant aquaporin structure. Furthermore, we report here, to our knowledge, the first structure of a heterologously expressed aquaporin in any eukaryotic species.

SoPIP2;1 was expressed both as His-tagged and as non-tagged protein in the methylotrophic yeast *Pichia pastoris*. These clones both express SoPIP2;1 variants at similarly high levels. When reconstituted into proteoliposomes and exposed to an osmotic gradient, recombinant SoPIP2;1 shows efficient water channel activity.[19]

Both His-tagged and non-tagged SoPIP2;1 could be reconstituted into several crystal forms. Although more different forms were obtained with the His-tagged protein (data not shown), better-ordered crystals resulted from non-tagged SoPIP2;1. We were interested in the native SoPIP2;1 in the spinach plasma membrane, and so we concentrated on the structural analysis of crystals reconstituted in the presence of lipids and the non-tagged protein. Non-tagged SoPIP2;1 crystallized in two forms. Tubular vesicles exhibited a specific surface texture, resulting from up-down oriented tetramers that are packed into alternating rows (data not shown). Image processing analysis revealed these crystals to be anisotropically ordered, and thus not suitable for high-resolution structural analysis. The second crystal type concerns membrane sheets that are mostly double-layered, exhibit $p4$ symmetry, and have lattice constants of $a=b=65$ Å. In contrast to the coaxially packed double-layered AQP0 crystals,[9,20] the two crystalline layers of SoPIP2;1 are shifted against each other by exactly half a unit cell in the x and y direction, and are thus packed in precise register as well. The crystallographic unit cell comprises a tetramer from one layer and four monomers from four neighboring tetramers in the opposing layer. Occasionally recorded single layers are generally less well ordered, suggesting that a stabilizing crystal contact exists between the two layers.

The crystal quality was assessed by electron diffraction at low electron dose (<5 é/Å^2). Strong diffraction spots could be observed to a resolution of 2.96 Å on untilted crystals and to 3.7 Å at a tilt angle of 60° (Figure 1). For structure determination

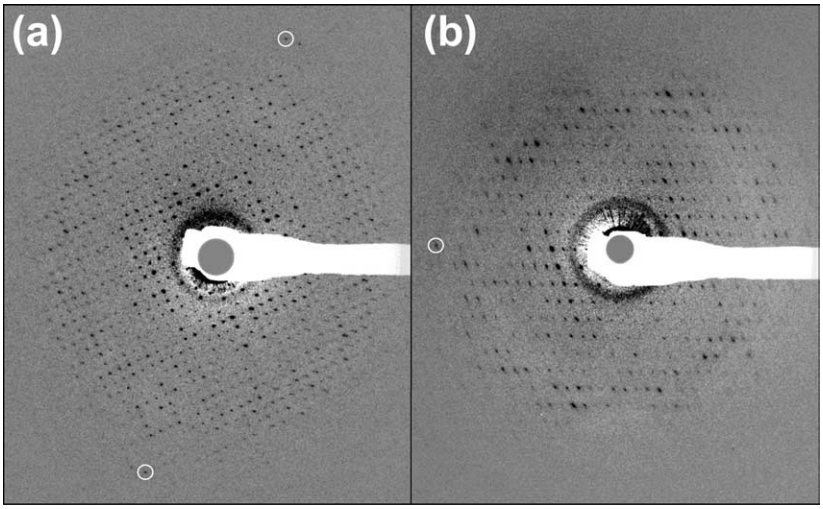

Figure 1. Electron diffraction of double-layered crystals at (a) 0° tilt and (b) 60° tilt. The circles in (a) indicate spots (16,15) corresponding to a resolution of 2.96 Å. In (b), the circle indicates spot (16,0) at a resolution of 3.7 Å. Crystal samples were embedded in 2% (w/v) glucose on molybdenum grids covered with a carbon film that was previously evaporated onto mica and floated on the grid. Electron diffraction patterns were recorded at low electron doses (<5 é/Å^2) on a Gatan 2K×2K CCD camera with a Philips CM200 FEG operated at 200 kV. The 2D crystals of OG-solubilized SoPIP2;1 were grown in the presence of *Escherichia coli* polar lipids at an LPR of 0.3 by dialysis for three days against a buffer containing 20 mM Tris–HCl (pH 8), 100 mM NaCl, 50 mM $MgCl_2$, 2 mM DTT, 0.03% (w/v) NaN_3.

high-resolution images of tilted specimens were collected and combined to obtain a 3D potential map (Table 1).

One tetramer and the complete unit cell are shown in Figure 2(a) and (b), respectively, with one monomer highlighted. Seven rod-like structures are clearly recognizable. By comparison with the atomic model of human AQP1,[21] they can be assigned to transmembrane helices 1–6 and loops B and E that form half-helices that fold back into the membrane to meet in the middle.[7] The remarkable arrangement of the two crystal layers stacked together by a tongue-and-groove fit of the extracellular surface, which is facilitated by the shift of one layer with respect to the other, is shown in Figure 2(c). This is radically different from the head-to-head coaxial packing of tetramers in the AQP0 double-layered crystals.[9]

The overall architecture of the channel has substantial similarity to AQP1, but some differences can be distinguished. The most remarkable difference is the length and straightness of helix 1. When compared to AQP1, helix 1 of SoPIP2;1 appears to protrude farther out from the extracellular membrane surface and to point towards the 4-fold axis of the tetramer (Figure 3(a) and (b)). A corresponding alteration is found for helix 2, which is more tilted at its N terminus than helix 2 of AQP1. All other helices fit well to the corresponding helices in AQP1. The visible differences in helices 1 and 2 dictate a different position of the connecting loop A in SoPIP2;1. In AQP1, this loop lies on top of helices 1 and 2, parallel with the side of the monomer. In the map of SoPIP2;1, however, the positions of the helix 1 C terminus and the helix 2 N terminus suggest that loop A is oriented towards the 4-fold center of the tetramer (Figure 3(a)). The tongue-and-groove packing arrangement results from the extracellular end of helix 1, which protrudes into the opposite layer, filling the gap between adjacent tetramers (Figure 2(b) and (c)). This suggests that the stability of the double-layered crystals might be the result of a contact between loops A from one layer with helices 3 and/or 6 of the opposing layer. Loop A in SoPIP2;1 is also different from that in AQP0, where tetramers are coaxially stacked face-to-face by prominent interactions between Pro38 in loop A, and a Pro–Pro motif (Pro109 and Pro110) in loop C.[9] It transpires that the crystalline packing of the two layers is, in both cases, dictated to a significant extent by the configuration of loop A.

Beside SoPIP2;1 and AQP0 a third aquaporin, AQP2, has been reported to preferably form double-layered two-dimensional crystals ordered to superior resolution.[22] In the case of AQP0,[9] this crystal form reflects the native state in the eye lens core, where AQP0 forms membrane junctions. AQP2 forms crystal contacts between the cytosolically located termini of the proteins and thereby differs from AQP0 and SoPIP2;1. The crystal packing of AQP2 is most probably not representing an *in vivo* situation but rather a crystallization artifact.[22] Whether the interactions of the extracellular parts of opposing SoPIP2;1 tetramers represent an *in vivo* situation has not been assessed. However, there are *in vivo* situations where different membrane domains of the plasma membrane of a cell are likely to interact *via* protein–protein interactions. Stomata closure and opening is accompanied by a substantial volume change of the guard cells. The membrane surface increase upon stomata opening cannot be explained by stretching of the plasma membrane.[23–25] It has to be attributed either to vesicles fusing with the plasma membrane or to plasma membrane invaginations being unfolded. Very fast cell volume changes necessitating vesicle fusion or invaginations unfolding have been recorded for mesophyll protoplasts isolated from leaf tissue.[26–28] Immunogold electron microscopy has demonstrated PIP subfamily members to be associated with plasmalemmasomes, invaginations of the plasma membrane protruding into the cytosol towards the central vacuole of *Arabidopsis* mesophyll cells.[29] It is possible that major integral proteins of the plasma membrane, such as

Table 1. Crystallographic data

Plane group symmetry	*p*4
Unit cell parameters	
$a=b$ (Å)	65
c (Å)	200 (assumed)
$\alpha=\beta=\gamma$ (deg.)	90
No. processed images	156 (0°, 21; 10°, 28; 15°, 16; 20°, 23; 30°, 37; 45°, 28; 60°, 3)
No. merged phases	24,479
Resolution limit for merging	5.0 Å (in the membrane plane; *x*,*y*-direction) 7.14 Å (perpendicular to the membrane plane; *z*-direction)
Phase residual (IQ-weighted) (deg.)	43.0 (overall) 34.4 (100–9.7 Å) 39.6 (9.7–6.9 Å) 50.6 (6.9–5.6 Å) 60.8 (5.6–5 Å)
Completeness[a] (%)	36.5 (resolution volume: 5 Å in *x*,*y*, 7.14 Å in *z*) 57 (resolution volume 6 Å in *x*,*y*, 7.14 Å in *z*) 65 (resolution volume 6 Å in *x*,*y*, 10 Å in *z*)

[a] Only reflections within the resolution volume having a figure of merit over 0.5 were included; the missing cone is comprised in this volume.

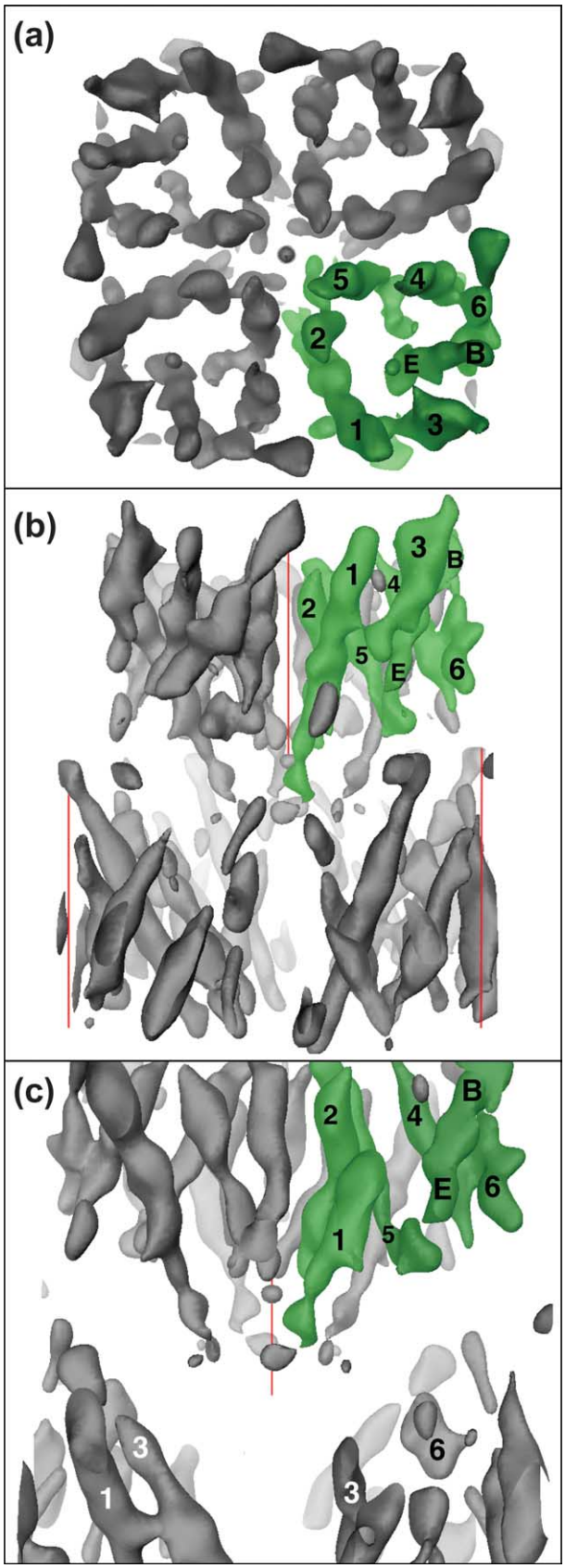

Figure 2. A 3D map of SoPIP2;1, calculated from 156 electron micrographs (see Table 1). (a) Cytosolic view of one tetramer. (b) Side-view of the unit cell comprising one tetramer and four monomers of the opposite layer. One monomer is highlighted in green. Helices 1–6 as well as loops B and E that fold back into the membrane and form a seventh transmembrane domain can be assigned as indicated. The 4-fold axes are drawn in red. (c) View into the center of the unit cell, where the extracellular ends of helices 1 from one tetramer protrude into the cleft between adjacent tetramers of the opposite layer. For clarity, parts of the map are cut away and the respective helices indicated. The map was calculated using the MRC software package.[32] Images were corrected for lattice distortions taking the Fourier-filtered images themselves as references. Measured phases and amplitudes were corrected for the tilted contrast transfer function and merged imposing *p*4 symmetry. Phase origins were refined and lattice lines for amplitudes and phases were fitted to create a 3D data set.

aquaporins, participate in interactions stabilizing membrane invaginations.

At the C terminus of loop A, PIPs exhibit a highly conserved Cys, which is not present in other aquaporin-like proteins in plants (Figure 3(c); U.J., unpublished results). Using the multiple sequence alignment reported by Heymann & Engel,[30] the conserved Cys of SoPIP2;1 was found to correspond to Thr44 in human AQP1 (Figure 3(c)). As displayed in Figure 3(a) and (b), the N-terminal part of the AQP1 helix 2 should be tilted towards the 4-fold axis to fit to the potential map of SoPIP2;1 in this region. The corresponding four Cys in SoPIP2;1 would then be remarkably close to each other, and close to the 4-fold axis of the tetramer. The high level of conservation suggests a special function for this Cys. According to their nearness, which is due to the particular configuration of loop A, these four Cys may stabilize the SoPIP2;1 tetramer by fostering hydrogen bonds or complexing a metal ion.

The particular arrangement of the four Cys was confirmed quantitatively by fitting helical segments to the 3D potential map of SoPIP2;1 using the program ROTTRANS.[31] In addition, the helical backbones of the atomic models of AQP1 and AQP0 in both open and closed conformation were fitted to the potential map of SoPIP2;1 and yielded cross-correlation scores of 0.37 (AQP1),[21] 0.366 (AQP0 open),[10] and 0.367 (AQP0 closed).[9] The question of whether the water channel of SoPIP2;1 is in an open or closed state cannot be answered at the resolution available. Differences are likely to be related to the conformation of single amino acid side-chains, such as the Tyr149 in AQP0.[9]

The high level of water permeability showed in activity measurements of proteoliposomes[19] suggests the water channels of SoPIP2;1 to be in an open conformation. However, the phosphorylation state of crystallized SoPIP2;1 is not known, and the mechanism of phosphorylation-mediated gating of the channel remains to be elucidated. The 2D crystals and the 3D map of the functional protein in a lipid bilayer provide a solid framework for this goal. As a result of the orientation of the tetramers within the double-layered crystals, the cytosolic C terminus as well as the B-loop are accessible for

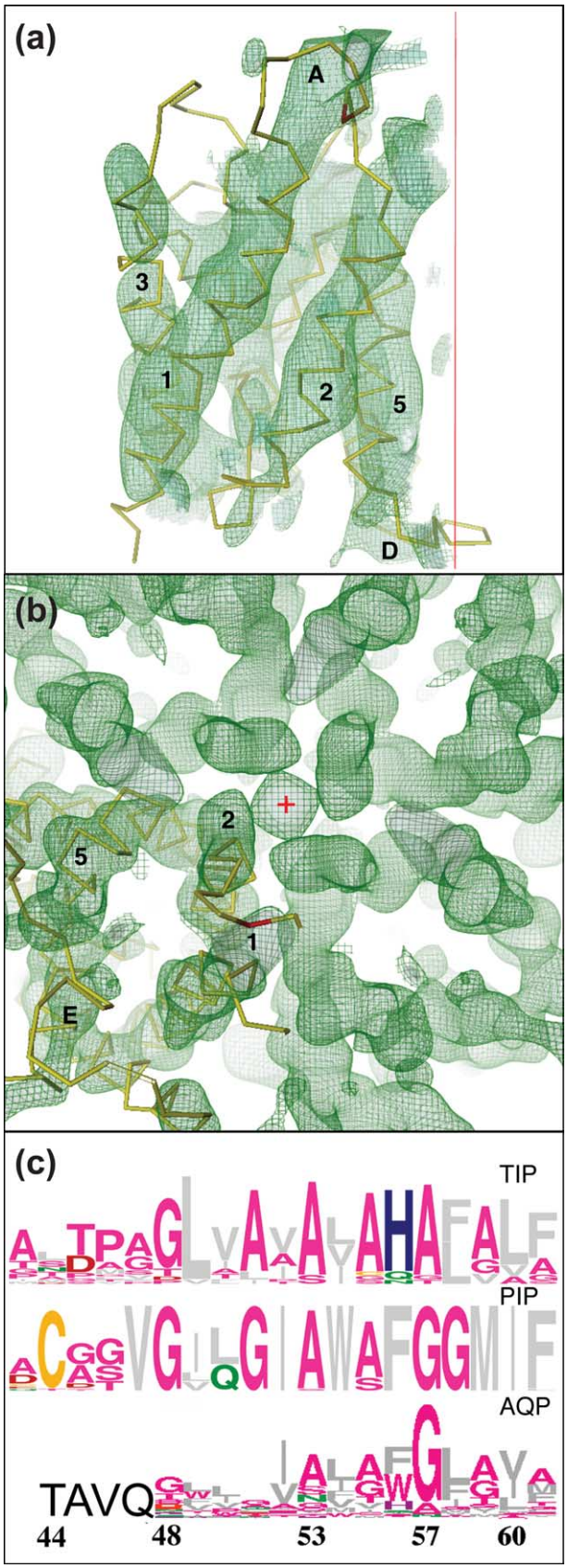

Figure 3. (a) Superposition of SoPIP2;1 potential map (green) with the C^{α} backbone of the atomic model of AQP1 (yellow); Thr44 is highlighted in red. The 4-fold axis is drawn in red in this side-view of the superimposed monomers, extracellular face up. (b) Extracellular view of a SoPIP2;1 tetramer with one AQP1 monomer fitted into a SoPIP2;1 monomer. The 4-fold center is indicated by a red cross. Superposition of the two structural datasets was performed using the program DINO (http://www.dino3D.org). (c) Alignment of the PIP and TIP consensus sequences of parts of loop A and helix 2 with the aquaporin consensus sequence of helix 2 (residues 48–61).[30] The PIP consensus sequence is based on SoPIP2;1 (AAA99274), all *Arabidopsis* PIPs,[2] maize PIPs,[33] and PIPs from *Picea abies* and *Physcomitrella patens* (CAB06080, CAB07783, AAS65964, translation of Physcobase contig 10071 http://moss.nibb.ac.jp/). The TIP consensus sequence is derived from *Arabidopsis*[2] and maize TIPs.[33] Sequence conservation is displayed by the sequence logos technique.[34,35] According to this alignment, the highly conserved Cys in PIPs corresponds to Thr44 in AQP1 (black letters).

phosphorylation experiments, allowing the channel to be resolved in the open and closed states.

References

1. Johansson, I., Karlsson, M., Johanson, U., Larsson, C. & Kjellbom, P. (2000). The role of aquaporins in cellular and whole plant water balance. *Biochim. Biophys. Acta*, **1465**, 324–342.
2. Johanson, U., Karlsson, M., Johansson, I., Gustavsson, S., Sjövall, S., Fraysse, L. *et al*. (2001). The complete set of genes encoding major intrinsic proteins in *Arabidopsis* provides a framework for a new nomenclature for major intrinsic proteins in plants. *Plant Physiol.* **126**, 1358–1369.
3. Chaumont, F., Barrieu, F., Wojcik, E., Chrispeels, M. & Jung, R. (2000). Plasma membrane intrinsic proteins from maize cluster in two sequence subgroups with differential aquaporin activity. *Plant Physiol.* **122**, 1025–1034.
4. Johansson, I., Larsson, C., Ek, B. & Kjellbom, P. (1996). The major integral proteins of spinach leaf plasma membranes are putative aquaporins and are phosphorylated in response to Ca^{2+} and apoplastic water potential. *Plant Cell*, **8**, 1181–1191.
5. Johansson, I., Karlsson, M., Shukla, V. K., Chrispeels, M. J., Larsson, C. & Kjellbom, P. (1998). Water transport activity of the plasma membrane aquaporin SoPIP2;1 is regulated by phosphorylation. *Plant Cell*, **10**, 451–459.
6. Kjellbom, P., Larsson, C., Johansson, I., Karlsson, M. & Johanson, U. (1999). Aquaporins and water homeostasis in plants. *Trends Plant Sci.* **8**, 308–314.
7. Murata, K., Mitsuoka, K., Hirai, T., Walz, T., Agre, P., Heyman, B. *et al*. (2000). Structural determinants of water permeation through aquaporin-1. *Nature*, **407**, 605–612.
8. Sui, H., Han, B. G., Lee, J. K., Walian, P. & Jap, B. K. (2001). Structural basis of water-specific transport through AQP1 water channel. *Nature*, **414**, 872–878.
9. Gonen, T., Sliz, P., Kistler, J., Cheng, Y. & Walz, T. (2004). Aquaporin-0 membrane junctions reveal the structure of a closed water pore. *Nature*, **429**, 193–197.
10. Harries, W. E., Akhavan, D., Miercke, L. J., Khademi, S. & Stroud, R. M. (2004). The channel architecture of aquaporin 0 at a 2.2-Å resolution. *Proc. Natl Acad. Sci. USA*, **101**, 14045–14050.

11. Fu, D., Libson, A., Miercke, L. J. W., Weitzman, C., Nollert, P., Krucinski, J. & Stroud, R. M. (2000). Structure of a glycerol-conducting channel and the basis for its selectivity. *Science*, **290**, 481–486.
12. Savage, D. F., Egea, P. F., Robles-Colmenares, Y., O'Connell, J. D., III & Stroud, R. M. (2003). Architecture and selectivity in aquaporins: 2.5 Å X-ray structure of aquaporin Z. *PloS Bio.* **1**, 334–340.
13. De Groot, B. L. & Grubmüller, H. (2001). Water permeation across biological membranes: mechanism and dynamics of aquaporin-1 and GlpF. *Science*, **294**, 2352–2356.
14. Tajkhorshid, E., Nollert, P., Jensen, M. O., Miercke, L. J., O'Connell, J., Stroud, R. M. & Schulten, K. (2002). Control of the selectivity of the aquaporin water channel family by global orientational tuning. *Science*, **296**, 525–530.
15. De Groot, B. L., Frigato, T., Helms, V. & Grubmüller, H. (2003). The mechanism of proton exclusion in the aquaporin-1 water channel. *J. Mol. Biol.* **333**, 279–293.
16. Chakrabarti, N., Tajkhorshid, E., Roux, B. & Pomes, R. (2004). Molecular basis of proton blockage in aquaporins. *Structure (Camb.)*, **12**, 65–74.
17. Chakrabarti, N., Roux, B. & Pomes, R. (2004). Structural determinants of proton blockage in aquaporins. *J. Mol. Biol.* **343**, 493–510.
18. Daniels, M. J., Chrispeels, M. J. & Yeager, M. (1999). Projection structure of a plant vacuole membrane aquaporin by electron cryo-crystallography. *J. Mol. Biol.* **294**, 1337–1349.
19. Karlsson, M., Fotiadis, D., Sjövall, S., Johansson, I., Hedfalk, K., Engel, A. & Kjellbom, P. (2003). Reconstitution of water channel function of an aquaporin overexpressed and purified from *Pichia pastoris*. *FEBS Letters*, **537**, 68–72.
20. Fotiadis, D., Hasler, L., Müller, D. J., Stahlberg, H., Kistler, J. & Engel, A. (2000). Surface tongue-and-groove contours on lens MIP facilitate cell–cell adherence. *J. Mol. Biol.* **300**, 779–789.
21. De Groot, B. L., Engel, A. & Grubmüller, H. (2001). A refined structure of human aquaporin-1. *FEBS Letters*, **504**, 206–211.
22. Schenk, A. D., Werten, P. J. L., Scheuring, S., de Groot, B. L., Müller, S. A., Stahlberg, H. *et al*. (2005). The 4.5 Å structure of human AQP2. *J. Mol. Biol*. In the press.
23. Blatt, M. R. (2000). Cellular volume control in stomatal movements in plants. *Annu. Rev. Cell Dev. Biol.* **16**, 221–241.
24. Geelen, D., Leyman, B., Batoko, H., Di Sansebastiano, G. P., Moore, I. & Blatt, M. R. (2002). The abscisic acid-related SNARE homolog NtSyr1 contributes to secretion and growth: evidence from competition with its cytosolic domain. *Plant Cell*, **14**, 387–406.
25. Pratelli, R., Sutter, J. U. & Blatt, M. R. (2004). A new catch in the SNARE. *Trends Plant Sci.* **9**, 187–195.
26. Ramahaleo, T., Morillon, R., Alexandre, J. & Lassalles, J. P. (1999). Osmotic water permeability of isolated protoplasts. Modification during development. *Plant Physiol.* **119**, 885–896.
27. Morillon, R., Lienard, D., Chrispeels, M. J. & Lassalles, J. P. (2001). Rapid movements of plants organs require solute–water cotransporters or contractile proteins. *Plant Physiol.* **127**, 720–723.
28. Moshelion, M., Moran, M. & Chaumont, F. (2004). Dynamic changes in the osmotic water permeability of protoplast plasma membrane. *Plant Physiol.* **135**, 2301–2317.
29. Robinson, D. G., Sieber, H., Kammerloher, W. & Schaffner, A. R. (1996). PIP1 aquaporins are concentrated in plasmalemmasomes of *Arabidopsis thaliana* mesophyll. *Plant Physiol.* **111**, 645–649.
30. Heymann, J. B. & Engel, A. (2000). Structural clues in the sequence of the aquaporins. *J. Mol. Biol.* **295**, 1039–1053.
31. de Groot, B. L., Heymann, J. B., Engel, A., Mitsuoka, K., Fujiyoshi, Y. & Grubmüller, H. (2000). The fold of human aquaporin 1. *J. Mol. Biol.* **300**, 987–994.
32. Crowther, R. A., Henderson, R. & Smith, J. M. (1996). MRC image processing programs. *J. Struct. Biol.* **116**, 9–16.
33. Chaumont, F., Barrieu, F., Wojcik, E., Chrispeels, M. J. & Jung, R. (2001). Aquaporins constitute a large and highly divergent protein family in maize. *Plant Physiol.* **125**, 1206–1215.
34. Crooks, G. E., Hon, G., Chandonia, J. M. & Brenner, S. E. (2004). WebLogo: a sequence logo generator. *Genome Res.* **14**, 1188–1190.
35. Schneider, T. D. & Stephens, R. M. (1990). Sequence logos: a new way to display consensus sequences. *Nucl. Acids Res.* **18**, 6097–6100.

Edited by W. Baumeister

(Received 18 February 2005; received in revised form 25 April 2005; accepted 2 May 2005)